2008

High-Order Discontinuous Galerkin Method for Boltzmann Model Equations

Alina A. Alexeenko
Purdue University - Main Campus, alexeenk@purdue.edu

Cyril Galitzine
Purdue University

Alexander M. Alekseenko
California State University

Recommended Citation
Alexeenko, Alina A.; Galitzine, Cyril; and Alekseenko, Alexander M., "High-Order Discontinuous Galerkin Method for Boltzmann Model Equations" (2008). *School of Aeronautics and Astronautics Faculty Publications.* Paper 12.
http://dx.doi.org/10.2514/6.2008-4256

40th Thermophysics Conference
23 - 26 June 2008, Seattle, Washington

AIAA 2008-4256

2008-4256

40th Thermophysics Conference, 21-26 June 2008, Seattle, WA

High-Order Discontinuous Galerkin Method for Boltzmann Model Equations

Alina A. Alexeenko*and Cyril Galitzine †

School of Aeronautics & Astronautics, Purdue University, West Lafayette, IN 47907.

Alexander M. Alekseenko‡

Department of Mathematics, California State University, Northridge, CA 91330.

High-order Runge-Kutta discontinuous Galerkin (DG) method is applied to the kinetic model equations describing rarefied gas flows. A conservative DG discretization of non-linear collision relaxation term is formulated for Bhatnagar-Gross-Krook and ellipsoidal statistical models. The numerical solutions using RKDG method of order up to four are obtained for two flow problems: the heat transfer between parallel plates and the normal shock wave. The convergence of RKDG method is compared with the conventional second-order finite volume method for the heat transfer problem. The normal shock wave solutions obtained using RKDG are compared with the experimental measurements of density and velocity distribution function inside the shock.

I. Introduction

Many practical applications in non-equilibrium gas dynamics require the kinetic description of gas flow phenomena that are governed by the Boltzmann kinetic equation. For applications involving unsteady rarefied gas flows, the direct simulation Monte Carlo method for stochastic solution of the Boltzmann equation may not be practical and the deterministic numerical solution of the Boltzmann-BGK equation can be more useful. However, the computational time and memory required for the deterministic kinetic modeling are large due to the multi-dimensionality of the Boltzmann-BGK equation whose phase space involves both velocity and spatial coordinates. Therefore, the development of high-order space/time discretization methods for the Boltzmann-BGK equation is very important.

Currently, there are two main approaches to obtaining high-order space/time discretization for solution of partial-differential equations. The first approach is based on weighted essentially non-oscillatory (WENO) finite volume and finite different methods. The WENO approach was first suggested in mid-1990s by Jiang and Shu[1] and is currently the most widely used high-order spatial reconstruction technique for Euler and Navier-Stokes equations.[2–4] The main idea of the WENO approach consists in applying an adaptive stencil for high-order reconstruction of values at cell boundaries using volume-averaged values. The stencil adaptation in WENO is based on a convex combination of all possible stencils with weights based on the local smoothness of the numerical solution. Recently, high-order WENO schemes for finite difference method has been applied for the solution of the Boltzmann-Poisson equation for simple rectangular geometries.[5]

Another class of high-order numerical methods is the Runge-Kutta discontinuous Galerkin (RKDG) finite element method. The RKDG method has been recently shown in Ref.[6] to have a significant advantage in computational efficiency over the WENO approach for a number of hyperbolic conservation laws but has not yet been applied for the Boltzmann equation. The discontinuous Galerkin method is the finite element method with a test space of piecewise-continuous functions that allows for discontinuities to exist at element boundaries. In the case when polynomials are used as the test functions, the order of the space discretization of the DG method is determined by the highest degree of the polynomial basis and can be implemented for

*Assistant Professor, AIAA Member. Email: alexeenk@purdue.edu

†Graduate Student, AIAA Student Member. Currently at the University of Michigan; email: cyrilg@umich.edu

‡Assistant Professor. Email: alexander.alekseenko@csun.edu

arbitrarily high-order accuracy away from the discontinuities. The time discretization is based on the Runge-Kutta schemes and has the same order as the DG method. The high-order implementation of the RKDG method for the Boltzmann equation requires a self-consistent high-order formulation of the collision term that also enforces the total mass, momentum and energy conservation. In this paper we present a self-consistent formulation of the discontinuous Galerkin method for the Boltzmann-BGK equation together with details of implementation and a comparison with the second-order finite volume method for one-dimensional heat transfer problem.

The Boltzmann equation has the form

$$\frac{\partial f}{\partial t} + \vec{u} \cdot \frac{\partial f}{\partial \vec{x}} = C\left(f\right) \tag{1}$$

where $\vec{x} = (x, y, z)$ and $\vec{u} = (u, v, w)$ are Cartesian coordinates in physical and velocity space, respectively, and $f = f(t, \vec{x}, \vec{u})$ is the velocity distribution function of molecules defined by the condition that $f(t, \vec{x}, \vec{u}) d\vec{u} d\vec{x}$ is the number of molecules at time t whose velocities lie between the limits $\vec{u}$ and $\vec{u}+d\vec{u}$ and whose coordinates lie between the limits $\vec{x}$ and $\vec{x} + d\vec{x}$. Here $C\left(f\right)$ is the collision term that can be approximated by a single-relaxation-time model in the form:

$$C\left(f\right) = \nu\left(f^{\mathrm{eq}} - f\right) \tag{2}$$

where ν is the collision frequency, and for the conventional BGK[7] model

$$f^{\mathrm{eq}} = f_M = n(t, \vec{x})(2\pi RT(t, \vec{x}))^{-3/2} \exp\left(-\frac{(\vec{u} - \vec{u}(t, \vec{x}))^2}{2RT}\right)$$

is the local equilibrium Maxwell-Boltzmann distribution function and n, T and $\vec{u}$ are the gas number density, temperature and bulk velocity given by:

$$n(t, \vec{x}) = \int f(t, \vec{x}, \vec{u}) d\vec{u} \tag{3}$$

$$n(t, \vec{x})\vec{u}(t, \vec{x}) = \int \vec{u} f(t, \vec{x}, \vec{u}) d\vec{u} \tag{4}$$

$$n(t, \vec{x})T(t, \vec{x}) = \frac{1}{3R} \int (\vec{u} - \vec{u})^2 f(t, \vec{x}, \vec{u}) d\vec{u} \tag{5}$$

For the ellipsoidal statistical model, f^{eq} is the anisotropic Gaussian:

$$f^{\mathrm{eq}} = \frac{\rho}{\sqrt{\det\left(2\ \pi\overline{\overline{\lambda}}\right)}} \exp\left(-\frac{1}{2}\left(\vec{u} - \vec{\vec{u}}\right) \overline{\overline{\lambda}}^{-1} \left(\vec{u} - \vec{\vec{u}}\right)\right) \tag{6}$$

where tensor $\overline{\overline{\lambda}}$ is a linear combination of the stress tensor $\overline{\overline{\sigma}} = \left(\vec{u} - \vec{\vec{u}}\right) \otimes \left(\vec{u} - \vec{\vec{u}}\right) f$ and the Maxwellian isotropic stress tensor $\theta\overline{\overline{I}} = \left(\vec{u} - \vec{\vec{u}}\right) \otimes \left(\vec{u} - \vec{\vec{u}}\right) f_M$,

$$\overline{\overline{\lambda}} = \frac{1}{Pr}\theta\overline{\overline{I}} + \left(1 - \frac{1}{Pr}\right)\overline{\overline{\sigma}} \tag{7}$$

with Pr being the correct Prandtl number, taken to be 2/3 for monatomic gases.

II. Numerical Method

II.A. Discretization in the Velocity Space

The standard technique of the discrete velocity method[8] is used to reduce the model Boltzmann equation to a series of hyperbolic partial differential equations in space and time. First, in order to reduce computational costs and simplify the implementation of the one dimensional problems, we recast Eq. (1) in terms of the two reduced distribution functions:[9]

$$f_1\left(u, x, t\right) = \int\int f\left(\vec{u}, \vec{x}, t\right) dvdw, \quad f_2\left(u, x, t\right) = \int\int v^2 f\left(\vec{u}, \vec{x}, t\right) dvdw \tag{8}$$

We then assume that a finite number of molecular velocities u^j, $j = 1, \ldots, N_1$ is selected in the x direction. By replacing the reduced distribution functions in the corresponding equations with the vectors $f_1^j(x,t) = f_1(u_j, x, t)$ and $f_2^j(x,t) = f_2(u_j, x, t)$, $j = 1, \ldots, N_1$, we arrive at the model describing the motion of a discrete velocity gas[10]

$$\frac{\partial}{\partial t} f_1^j(x,t) + u^j \frac{\partial}{\partial x} f_1^j(x,t) = C_1^j(f) \tag{9}$$

$$\frac{\partial}{\partial t} f_2^j(x,t) + u^j \frac{\partial}{\partial x} f_2^j(x,t) = C_2^j(f) \tag{10}$$

where functions $C_p^j(f) = \nu\left(f_p^{\mathrm{eq}} - f_p^j\right)$, $p = 1, 2$ are the discrete velocity collision operators whose exact formulas depend on the selected integration quadratures in the discrete velocity space. The partial differential equations (9) and (10) are then solved numerically.

Note that the employed discrete velocity method is a straightforward and currently the most widely used technique for discretization in velocity space. Although the method can be easily implemented and results in a symmetric hyperbolic system of equations, this technique, however, has a significant drawback. The conservation laws which depend on the discretization in the velocity space, including the conservation of mass, momentum and energy, are satisfied only approximately in the discrete velocity approximation. It was indicated previously[11] that using the Gauss type formulas for integration in the velocity space can solve the problem only partially. To achieve the conservation properties on the round-off level, the discrete equilibrium distribution function has been suggested by Mieussens.[11] A generalization of the approach of Mieussens[11] to the high-order DG approximation is described in Section II.C. It also seems interesting to implement the higher order discretization in the velocity space using, for example, the spectral representation of the distribution function. The development of such methods is underway and will be discussed in the future works.

II.B. Discontinuous Galerkin Formulation

To discrete approximation of the Boltzmann-BGK equation in the spatial variables is done by DG methods. Let the interval $[0, L]$ in x direction be divided into N elements, $I_i = \{x_{i-1/2} \le x \le x_{i+1/2}\}$, $i = 1, \ldots, N$, where $x_{1/2} = 0$ and $x_{N+1/2} = L$. On each I_i we will seek a solution in the form of an expansion over the orthogonal basis of the unassociated Legendre polynomials of degrees from 0 to k:

$$f_p^j(x,t)\Big|_{I_i} = \sum_{m=1}^{k+1} \phi_{m,i}(x) F_{i,m}^{j,p}(t) \tag{11}$$

where $\phi_{m,i} = P_m(2(x - x_i)/\Delta x_i)$, $x_i = (x_{i+1/2} + x_{i-1/2})/2$, $\Delta x_i = x_{i+1/2} - x_{i-1/2}$ and $P_m(x)$ is the m^{th} Legendre's polynomial.

Following the standard techniques of the finite element formulations and by using the properties of the unassociated Legendre polynomials, the weak formulation of Eq. (9) and (10) can be expressed as

$$\frac{\Delta x_i}{2m+1} \frac{d}{dt} F_{i,m}^{j,p}(t) + H_{i+1/2}^{j,p} - (-1)^k H_{i-1/2}^{j,p} - u^j \sum_{l=0}^{k} K_{lm} F_{i,m}^{j,p} = R_{i,m}^{j,p} \tag{12}$$

where $H_{i+1/2}^{j,p}$ denotes the numerical flux between the cells I_i and I_{i+1} and the matrix K_{lm} is defined by

$$K_{lm} = \int_{I_i} \phi_{l,i}(x) \phi_{m,i}'(x) dx \tag{13}$$

The discretized collision operator $R_{i,m}^{j,p}$ is discussed in detail in the next section.

Various flux approximations are available[12] and here the Godunov flux is used

$$H_{i+1/2}^{j,p} = \begin{cases} u^j f_p^j|_{I_{i+1}}\left(x_{i+1/2}, t\right) & \text{if } u^j \le 0 \\ u^j f_p^j|_{I_i}\left(x_{i+1/2}, t\right) & \text{if } u^j > 0 \end{cases} \tag{14}$$

The resulting system of ODEs is integrated in time by Runge-Kutta methods. Based on numerical results of Ref.,[13] the order of the Runge-Kutta method must be chosen at least $k+1$. The formulas for practical total

variation diminishing (TVD) Runge-Kutta schemes are given in Ref.[14] for $k \leq 5$. The numerical stability is achieved if the CFL number based on the maximum absolute value of u^j is less than 1 (for $k = 0, 1$), and less than 2/3 for k=2. The maximum CFL numbers for higher-order TVD Runge-Kutta schemes are smaller and are given in Ref.[14] Due to the effect of the collision term an *a priori* estimate for the maximum allowable CFL number for a given time and space discretization order is not possible. The maximum time step for each case was thus instead determined by numerical experimentation.

II.C. Conservative Discretization of the Collision Term

An approximation of the collision relaxation term in the kinetic model equation is formulated for the DG method such that the mass, momentum and energy conservation is enforced. The collision relaxation term has the form:

$$R_{p,i}^{m,j} = \int_{I_i} \nu(x) \left(f_p^{j,\mathrm{eq}} - \sum_{l=0}^{k} \phi_{l,i}(x) F_{i,l}^{j,p}(t) \right) \phi_{m,i}(x) dx \tag{15}$$

In order to complete the discontinuous Galerkin formulation, we need to specify how the discrete equilibrium distribution functions $f_p^{j,\mathrm{eq}}$ can be found. On each cell I_i the discrete distribution functions $f_{\mathbf{d}}^{\mathrm{eq}} = \left\{ f_{1,d}^{j,\mathrm{eq}}, f_{2,d}^{j,\mathrm{eq}} \right\}_{j=1}^{N_1}$ are defined by the relations

$$f_1^{j,\mathrm{eq}} = \exp\left(a_1(x) + a_2(x) u^j + a_3(x) (u^j)^2 \right), \quad f_2^{j,\mathrm{eq}} = -\frac{1}{2\, a_4^j(x)} f_1^{j,\mathrm{eq}} \tag{16}$$

The conservation properties of the discrete collision operator are achieved by specifying the condition that the discrete equilibrium distribution function $f_{\mathbf{d}}^{\mathrm{eq}}$ satisfies the same conditions on moments as its equivalent in continuous velocity space, i.e.,

$$\langle f_{\mathbf{d}}^{\mathrm{eq}} \rangle_{\mathbf{d}} = \langle f^{eq} \rangle \tag{17}$$

$$\langle \vec{u_{\mathbf{d}}}\, f_{\mathbf{d}}^{\mathrm{eq}} \rangle_{\mathbf{d}} = \langle \vec{u}\, f^{eq} \rangle \tag{18}$$

$$\langle \vec{u_{\mathbf{d}}} \otimes \vec{u_{\mathbf{d}}}\, f_{\mathbf{d}}^{\mathrm{eq}} \rangle_{\mathbf{d}} = \langle \vec{u} \otimes \vec{u}\, f^{eq} \rangle \quad . \tag{19}$$

where $\langle \rangle_{\mathbf{d}}$ and $\langle \rangle_{\mathbf{d}}$ denote, respectively, integration over the discrete and continuous velocity space. If the functions $a_q(x)$, $q = 1, \ldots, 4$ can be found to such that the discrete identities (17)–(19) are satisfied, the discrete collision term does not give rise to any source or sink of mass, momentum or energy.

In order to be consistent with the weak formulation of the DG method and to retain high order accuracy the weak formulation of Eq. (17) to (19) is used

$$\int_{I_i} \nu \left(\sum_{j=1}^{N_1} (u^j)^s f_{1,d}^{j,eq} - \langle (u_x)^s f_1^{eq} \rangle \right) \phi_{m,i}\, dx = 0 \quad 0 \leq s \leq 2 \tag{20}$$

$$\int_{I_i} \nu \left(\sum_{j=1}^{N_1} f_{2,d}^{j,eq} - \langle f_2^{eq} \rangle \right) \phi_{m,i}\, dx = 0 \qquad 0 \leq m \leq k \tag{21}$$

The coefficients a_q in Eq. (16) are sought in the form

$$a_q(x) = \sum_{m=0}^{k} A_{q,m}\, \phi_{m,i}(x) \tag{22}$$

which does indeed ensure, that the discrete collision term $C(f_{\mathbf{d}}) = \nu(f_d - f_d^{eq}(f_{\mathbf{d}}))$ does not give rise to any source or sink of mass momentum or energy. The difference between this form and the one used in the finite-volume method is that for discontinuous Galerkin method with $k > 0$ the collision frequency, number density, bulk velocity and temperature vary inside the element I_i.

The collision frequency $\nu(x)$ is calculated as

$$\nu(x) = Pr \frac{n(x) k T(x)}{\mu(x)} \quad \text{where} \quad \frac{\mu(x)}{\mu_{ref}} = \left(\frac{T(x)}{T_{ref}} \right)^{\omega}$$

This yields for each cell I_i a system of $4 \times (k+1)$ non-linear equations for $\{A_{1 \leq p \leq 4, 1 \leq m \leq k+1}\}$ that is solved using Newton's method.

III. Results and Discussion

Below we present the results of numerical calculations using the discontinuous Galerkin method described above. The DG methods of third and fourth order are applied for the solution of the Boltzmann-BGK equation for 1D heat transfer and normal shock wave problems.

III.A. 1D Heat Transfer

The conditions are as follows: two plates at temperatures of 79 K and 294 K are separated by the distance of 2.28 cm. Argon gas fills the gap between the plates and is initially at the density of 1.785×10^{-5} kg/m^3. The Knudsen number based on this number density and the gap distance is about 0.075. These conditions correspond to conditions in Fig. 7 of Ref.[15] The wall boundary conditions is the fully diffuse reflection.

Here we compare the numerical results obtained by the second-order finite volume method (FVM-2)(described in detail, for example, in Ref.[16]) and the Runge-Kutta discontinuous Galerkin method with k=2 and 3 which corresponds to third (RKDG-3) and fourth (RKDG-4) order, respectively. All results presented in this section are for steady-state which was obtained by iterating in time until the time convergence is reached. The time convergence criteria is that the L_2 norm of residual decreases by a factor of 10^6. All calculations were done in double precision (REAL*8) on an AMD Opteron 252 2.6GHz.

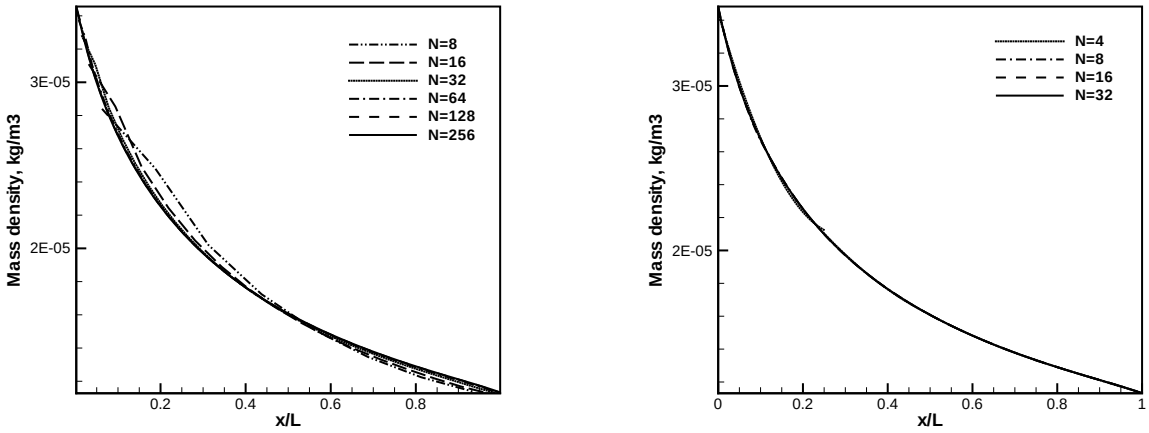

Figure 1. Gas density for FVM-2 (left) and RKDG-3 (right).

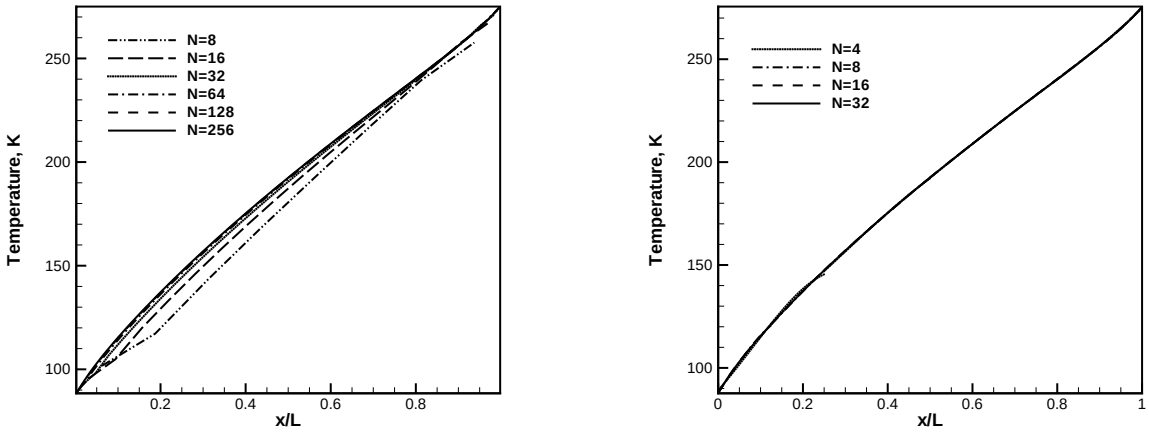

Figure 2. Gas temperature for FVM-2 (left) and RKDG-3 (right).

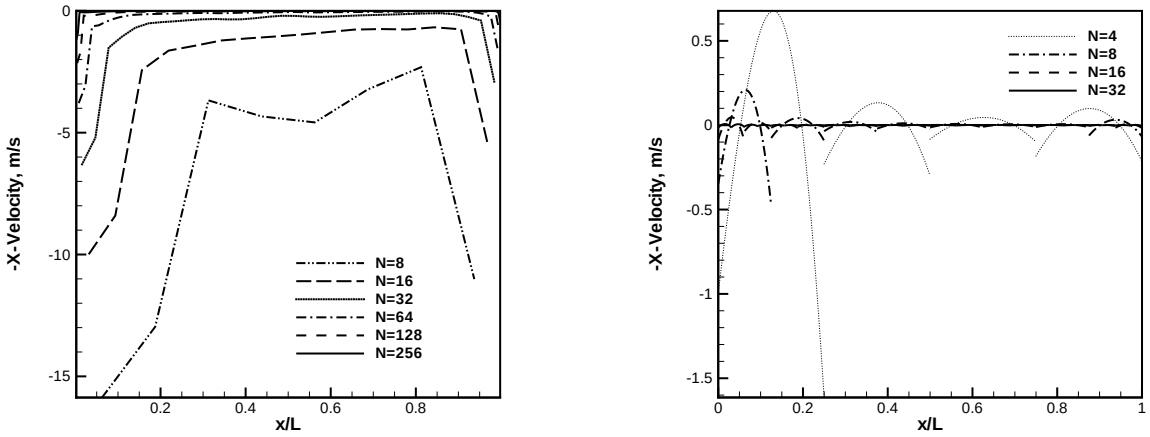

Figure 3. Gas velocity for FVM-2 (left) and RKDG-3 (right).

Table 1. Computational parameters for FVM-2 method

Case	Δt, sec	# of iterations	CPU time, sec	T($\frac{x}{L}$=0.5), K
N=8	2E-2	1431	0.088	180.532
N=16	1E-2	3188	0.388	187.241
N=32	5E-3	6702	1.62	190.526
N=64	2.5E-3	13476	6.54	191.847
N=128	1.25E-3	26503	25.86	192.305
N=256	6.25E-4	52022	107.1	192.447
N=512*	3.125E-4	93082	433.135	192.497

*This case only converged to residual of about 5×10^{-6} due to round-off errors.

The calculated mass density, temperature and bulk velocity are plotted in Figures 1-3 for different values of N, the number of finite volumes or elements along X. The RKDG-3 and RKDG-4 results are the local values of macroparameters at 256 uniformly distributed points. The FVM-2 results for mass density and temperature converge to the third significant digit for $N = 128$ and larger, while the RKDG-3 results are converging up to the four significant digits for $N = 8$ and larger. The bulk velocity values calculated by the FVM-2 and RKDG-3 methods show larger deviation from the exact solution (zero bulk velocity at steady-state) than the mass density and temperature.

For comparison of the computational efficiency of the methods, the time step, number of iterations and total CPU times are listed for these two methods in Tables 1-4. The Runge-Kutta discontinuous Galerkin method in general is much more CPU intensive (about 12 times) that the second-order finite-volume method for the same N. The most computationally intensive part of the RKDG solution of the Boltzmann-BGK equation is the calculation of collision relaxation term. This is due to the fact that the non-linear system of equations has to be solved iteratively and this portion of the algorithms requires an order of $O((k+1)^3 \times N \times N_1)$ operations. Non-conservative schemes that retain the order of accuracy of space and time discretization can be constructed which are much more faster but they should be used with caution.

Based on the comparison of mass density, temperature and bulk velocity convergence, the RKDG-3 solution with N=8 is at least as good as FVM-2 solution with N=128. The CPU time required to obtain RKDG-3 solution with N=8 is about 2.5 times smaller than that for the FVM-2 solution with N=128. The required memory is about 5 times smaller. In general, based on this comparison one can conclude that third-order Runge-Kutta discontinuous Galerkin solution for the Boltzmann-BGK equation requires significantly less memory and CPU time than a second-order finite-volume method with the same accuracy. The scaling

Table 2. Computational parameters for RKDG-2 method

Case	Δt, sec	# of iterations	CPU time, sec	T($\frac{x}{L}$=0.5), K
N=4	4E-2	894	0.376	194.005, 193.670
N=8	2E-2	1740	1.432	192.957, 192.875
N=16	9E-3	3720	5.952	192.613, 192.607
N=32	4E-3	8151	25.34	192.531, 192.532
N=64	1.9E-3	16771	102.56	192.509, 192.510
N=128	0.9E-3	33656	404.58	192.503, 192.503

Table 3. Computational parameters for RKDG-3 method

Case	Δt, sec	# of iterations	CPU time, sec	T($\frac{x}{L}$=0.5), K
N=4	2.9E-2	1210	2.47	192.142, 192.487
N=8	1.3E-2	2540	10.24	192.476, 192.511
N=16	5.7E-3	5642	45.24	192.5, 192.505
N=32	2.5E-3	12273	193.98	192.501, 192.502
N=64	1.2E-3	24772	784.08	192.5, 192.5

Table 4. Computational parameters for RKDG-4 method

Case	Δt, sec	# of iterations	CPU time, sec	T($\frac{x}{L}$=0.5), K
N=2	4.6E-2	765	1.97	195.157, 193.083
N=4	2.25E-2	1476	7.45	192.518, 192.505
N=8	0.9E-2	3585	35.55	192.504, 192.503

of CPU time and memory is expected to be similar in a two-dimensional case as in the one-dimensional calculations due to the fact that the number of elements and basis functions increase in the same manner with the dimensionality of the problem.

Results obtained using fourth-order RKDG method are listed in Table 4. It can be seen that RKDG-4 method is not more efficient than the RKDG-3 due to the fact that smaller time steps are required for stability of the fourth-order Runge-Kutta scheme.

III.B. Normal Shock Wave

A strong shock wave in Argon at Mach number of 7.183 was calculated using RKDG methods of order up to four. The conditions correspond to the experimental measurements of number density and distribution function obtained by Muntz and Holtz.[17] The viscosity coefficient at the reference temperature $T_{ref} = 273.2$ K was assumed to be $\mu_{ref} = 2.117 \times 10^{-5} kg/(m \cdot s)$. The viscosity-temperature exponent $w = 0.72$ was used to calculate the power-law dependence of viscosity on temperature, $\mu = \mu_{ref} \left(\frac{T}{T_{ref}}\right)^w$. This value of w is based on the detailed comparison of DSMC simulations using the variable-hard-sphere model with experimental measurements.[18]

First, we compare numerical solutions of the shock wave problem using RKDG shemes of various orders. To illustrate the influence of the order of the method and grid size on convergence and solution accuracy, computational parameters such as the number of iterations, the total CPU time and error are shown in Table III.B. The quality of the solution obtained in phase is evaluated by the following error norm:

$$\|e\|_{l^2} = \left\langle \left(\int_0^L \left(f_1 - f_1^{\text{exact}} \right)^2 dx \right)^{1/2} \right\rangle_{\mathbf{d}}.$$

The local convergence of the solution can also be evaluated by a macroparameter value at a specific location. In this case we choose the translational temperature at the location where the normalized number density, $\hat{h} = \dfrac{n - n_1}{n_2 - n_1}$ is equal to 0.5. It can be seen that RKDG solutions of various orders converge to the value of $\tilde{T}(\tilde{n}) = 0.5) = 0.90248$. For example, to converge within the first four significant digits the second-order scheme (k=1) takes $N = 256$ elements, whereas the fourth-order scheme (k=3) takes only $N = 32$ elements. The CPU time required to obtain such converged solution is about 7 times less for the fourth-order scheme compared to the second-order one.

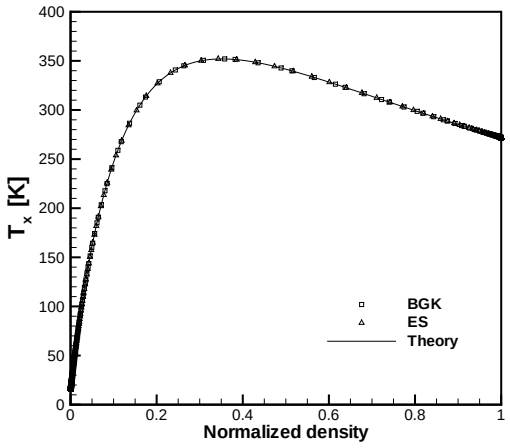

Figure 4. Comparison of calculated T_x with theory.[19]

The conservative character of the scheme was also checked by comparing the calculated streamwise temperature T_x with the theoretical value that can be obtained via conservation arguments as a function of n and upstream conditions.[19] The comparison is shown in Figure 4. Figure 5 shows the comparison between

Table 5. Influence of order and grid on solution with $N_1 = 32$ and $L = 0.25$e-1 m.

N	k	CFL	# of iterations	CPU time [s]	$\|e\|_{l^2}$	$\hat{T}(\hat{n}) = 0.5)$
8	0	0.9	9,634	2.31	2.3076984134986201e-01	0.677424
	1	0.6	39,449	42.97	1.0911501915247913e-01	0.896358
	2	0.45	60,058	215.27	1.531709655989704e-02	0.898842
	3	0.35	84,514	686.95	6.158115400889794e-03	0.903816
16	0	0.7	30,906	14.41	1.513344230391965e-01	0.857135
	1	0.7	77,693	165.74	2.279402506331994e-02	0.898871
	2	0.45	127,697	903.44	3.783026645272823e-03	0.903929
	3	0.30	189,853	2988	1.518325421092819e-03	0.901550
32	0	1.4	70,852	65.04	8.533108824098767e-02	0.565754
	1	0.6	187,380	783.8	5.352550042866056e-03	0.904059
	2	0.4	280,772	3,905.	7.123258202411460e-04	0.902181
	3	0.25	448,922	13,347.	2.716636632271850e-04	0.902485
64	0	1.35	157,524	299.37	4.186805626133487e-02	0.857710
	1	0.55	415,196	3,462.7	1.356570471677280e-03	0.902755
	2	0.30	747,084	20,606.	1.142634582580130e-04	0.902478
	3	0.20	1,179,000	69,499.	6.025242048653706e-05	0.902479
128	0	1.3	336,433	1,276.	2.063275407078794e-02	0.899794
	1	0.45	975,000	16,450.	3.405081958091302e-04	0.902555
	2	0.28	1,602,026	93,574.	1.114552952970969e-05	0.902475
	3	0.18	2,491,677	306,447.	–*	0.902480
256	1	0.45	2,565,495	91,810.	6.918037058537020e-05	0.902512

* f_1^{exact} obtained with $(N, k) = (128, 3)$

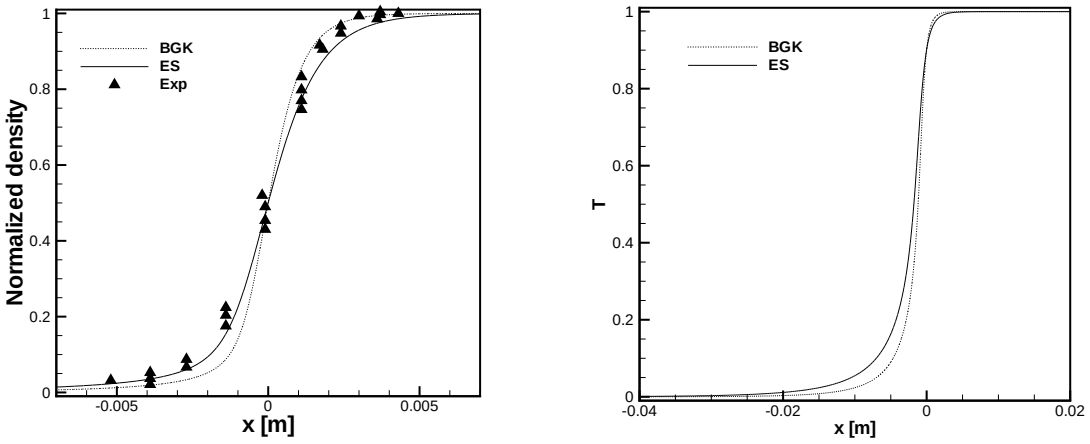

Figure 5. Normalized number density $\frac{n-n_1}{n_2-n_1}$ and temperature $\frac{T-T_1}{T_2-T_1}$ for Argon shock wave at M=7.183. Experimental data are from Holtz.[17]

the normalized number density and temperature obtained via the BGK and ES models. Experimental data for the number density taken from[17] are also shown. In order to obtain high quality numerical results a large domain domain size ($L = 0.150$ m) was chosen which was discretized with 512 elements using $(k, rk) = (2, 3)$ with 96 discrete velocities. The large number of discrete velocities is essential in getting an accurate solution due to the low-order discretization in the velocity space. The use of BGK model which corresponds to a larger Prandtl number results in overprediction of the shock wave thickness. The agreement between the calculated number density for ES model and experimental measurements is improved compared to BGK model.

Reduced distribution f_1 is shown in Figures 6 and 7 at several streamwise locations corresponding to normalized density values for which experimental data are available.[17] The distribution function f_1, however, has to be convolved with the window function of the measurement instrument in order to be compared with the data presented in[17] where details of the convolution procedure can be found.

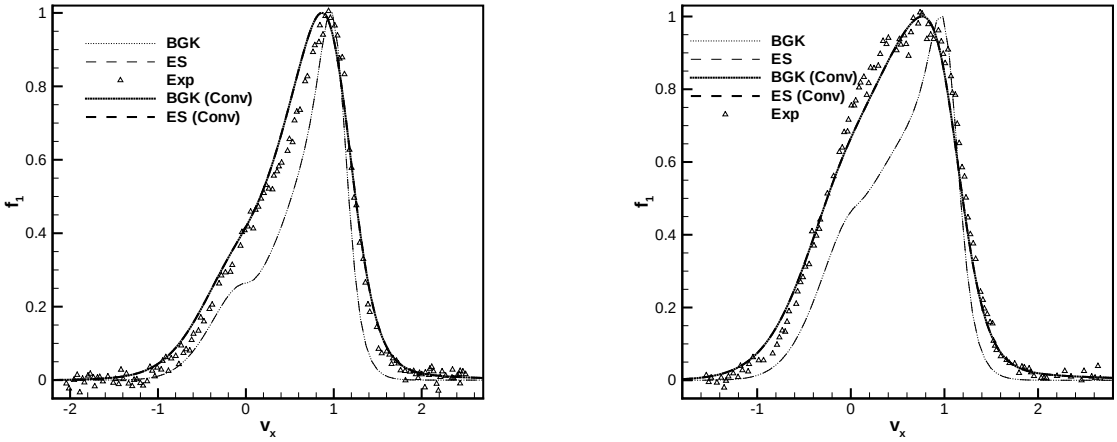

Figure 6. Comparison of calculated and experimentally measured[17] parallel velocity distribution function at $\tilde{n}$ =0.240 and 0.333.

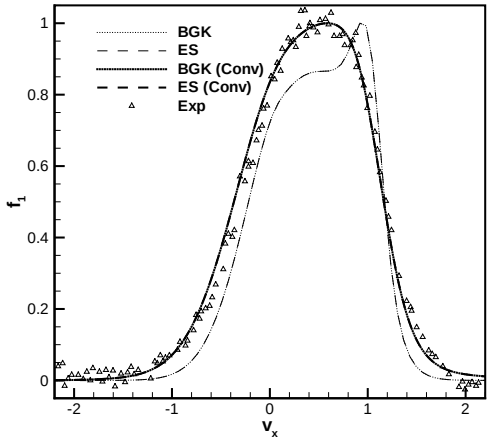

Figure 7. Comparison of calculated and experimentally measured[17] parallel velocity distribution function at $\tilde{n} = 0.433$.

As can be seen from the comparison in Figures 6-7, the BGK and ES models reproduce the experimentally measured distribution function shapes quite well. The difference between the two solutions is limited to the spatial variation of normalized density. Previously, large deviations of the measured and calculated distribution function have been reported. We attribute these deviations to the use of different viscosity

model, $w = 1$ instead of a more accurate value of 0.7, and limitations of the numerical solution in terms of velocity and spatial grid resolution.

IV. Conclusions

Conservative, high-order Runge-Kutta discontinuous Galerkin (RKDG) discretization of non-linear Boltzmann model kinetic equations is presented. The numerical solutions using RKDG method of order up to four are obtained for one-dimensional heat transfer problem and a strong shock wave in argon. The convergence of RKDG method is much faster as compared with the conventional second-order finite volume scheme. For the heat transfer problem, RKDG method of the third-order requires about 5 times less CPU time as compared with the second order finite volume method. The normal shock wave solutions of ES kinetic model obtained using RKDG agree well with the experimental measurements of density and velocity distribution function.

Acknowledgments

The authors would like to thank Natalia Gimelshein (ERC Inc., Edwards AF Base), Dr. Sergey Gimelshein (USC) and Dr. Ingrid Wysong (AFRL, Edwards, CA) for useful discussions. The computations reported in this paper were performed on 16 CPU Sunfire 4600 awarded through Sun Microsystems, Inc. Academic Excellence Grant award #EDUD-7824-070336-US. AA would like to acknowledge support from ASEE/Air Force Summer Faculty Fellowship program.

References

[1]Jiang, G. and Shu, C. W., "Efficient Implementation of Weighted Essentially Non-Oscillatory Schemes," *J. Computational Physics*, Vol. 126, 1996, pp. 202–228.

[2]Shi, J., Zhang, Y.-T., and Shu, C. W., "Resolution of high order WENO schemes for complicated flow structures," *J. Comput. Phys.*, Vol. 186, No. 2, 2003, pp. 690–696.

[3]Greenough, J. A. and Rider, W. J., "A quantitative comparison of numerical methods for the compressible Euler equations: fifth-order WENO and piecewise-linear Godunov," *J. Comput. Phys.*, Vol. 196, No. 1, 2004, pp. 259–281.

[4]Lee, T., Zhong, X., Gong, L., and Quinn, R., "Hypersonic Aerodynamic Heating Prediction Using Weighted Essentially Nonoscillatory Schemes," *J. of Spacecraft and Rockets*, Vol. 40, No. 2, 2003, pp. 294–298.

[5]Carrillo, J., Gamba, I., Majorana, A., and Shu, C., "2D semiconductor device simulations by WENO-Boltzmann schemes: efficiency, boundary conditions and comparison to Monte Carlo methods," *J. Comput. Phys.*, Vol. 214, No. 1, 2006, pp. 55–80.

[6]Zhou, T., Li, Y., and Shu, C. W., "Numerical Comparison of WENO Finite Volume and Runge-Kutta Discontinuous Galerkin Methods," *J Sci. Computing*, Vol. 16, No. 2, 2001, pp. 145–171.

[7]Bhatnagar, P. L., Gross, E. P., and Krook, M., "A Model for Collision Processes in Gases. I. Small Amplitude Processes in Charged and Neutral One-Component Systems," *Phys. Rev.*, Vol. 94, No. 3, 1954, pp. 511–525.

[8]Goldstein, D., Sturtevant, B., and Broadwell, J. E., "Investigations of the motion of discrete-velocity gases," *Rarefied Gas Dynamics: Theoretical and Computational Techniques*, AIAA, 1989, pp. 100–117.

[9]Giddens, D. P., Huang, A. B., and Young, V. Y. C., "Evaluation of Two Statistical Models Using the Shock Structure Problem," *Physics of Fluids*, Vol. 14, No. 12, 1971, pp. 2645–2651.

[10]Broadwell, J. E., "Study of rarefied shear flow by the discrete velocity method," *J. Fluid Mech.*, Vol. 19, 1964, pp. 401–414.

[11]Mieussens, L., "Discrete Velocity Models and Numerical Schemes for the Boltzmann-BGK Equation in Plane and Axisymmetric Geometries," *J. Comp. Phys.*, Vol. 162, 2000, pp. 429–466.

[12]Leveque, R., *Finite Volume Methods for Hyperbolic Problems*, Cambridge, 2002.

[13]Cockburn, B., "An introduction to the discontinuous Galerkin method for convection-dominated problems," *High-Order Methods for Computational Physics*, edited by T. B. Deconink, Vol. 9 of *Lecture Notes in Comput. Sci. Eng.*, Springer-Verlag, 1999, pp. 69–224.

[14]Shu, C.-W. and Osher, S., "Efficient implementation of essentially non-oscillatory shock- capturing schemes," *J. Comput. Phys*, Vol. 77, 1988, pp. 439–471.

[15]Wadsworth, D., "Slip effects in a confined rarefied gas. I: Temperature slip," *Phys. Fluids*, Vol. 5, 1993, pp. 1831.

[16]Mieussens, L. and Struchtrup, H., "Numerical comparisons of Bhatnagar-Gross-Krook models with proper Prandtl number," *Phys. Fluids*, Vol. 16, No. 8, 2004, pp. 2797–2813, BGK.

[17]Holtz, T., *Measurement of Molecular Velocity Distribution Functions in an Argon Normal Shock Wave at Mach Number 7*, Ph.D. thesis, University of Southern California, Jan. 1974.

[18]Erwin, D. A., Pham-Van-Diep, G. C., and Muntz, E. P., "Nonequilibrium gas flows. I: A detailed validation of Monte Carlo direct simulation for monatomic gases," *Phys. Fluids A*, Vol. 3, No. 4, 1991, pp. 697–705.

[19]Yen, S.-M., "Temperature Overshoot in Shock Waves," *Phys. Fluids*, Vol. 9, 1966, pp. 1417–1418.